



Quality control and nondestructive tests in MMC

MMC-Assess Thematic Network



Volume 5



Quality control and nondestructive tests in metal matrix composites

Y. D. Huang*, L. Froyen, M. Wevers

Department Metaalkunde en Toegepaste Materiaalkunde (MTM), Katholieke Universiteit Leuven, Kasteelpark Arenberg 44, B-3001 Heverlee, Belgium

1 Abstract

Quality control during fabrication and failure monitoring during service have gained importance in the field of metal matrix composites because of their growing uses, especially for structural applications. This review aims to provide a survey of quality control and nondestructive testing relevant to metal matrix composites. The first part presents the determination of the reinforcement parameters which play a very important role in controlling the performance of metal matrix composites. The second part describes the main relevant nondestructive techniques used to identify the defects produced during fabrication or in service. It also shows that the validation of nondestructive techniques and the relationship between their results and component performance should be particularly emphasized in future research work on metal matrix composites.

Keywords: Metal matrix composite, defects, nondestructive test, ultrasonics, acoustic emission, radiography, thermography, eddy current, low frequency vibration, scanning acoustic microscopy, noncontacting electromagnetic acoustic transducers

2 Introduction

Metal matrix composites (MMCs) offer a number of property advantages over conventional metal materials and alloys. In these composites one constituent is a metal or alloy forming at least one percolating network. The other constituent is embedded in this metal matrix and usually serves as reinforcement, which is normally a ceramic such as SiC and Al₂O₃. Their properties can be tailored by varying the constituents and their volume fractions. MMCs may be classified into four types according to the type of reinforcement: MMCs reinforced with particles (PRM), MMCs reinforced with whiskers or short fibers (SFRM), MMCs reinforced with continuous fibers (CFRM) and MMCs reinforced with mono-filaments (MFRM). For more information about MMCs one is referred to various publications which deal with materials science and micro-mechanics. (1-6)

In the past few years, MMCs have become realistic candidates for engineering components, such as automotive drive shafts, high speed train brake rotors and aero-engine components. Quality control during their fabrication routes and failure monitoring during their service are therefore recognized as very important. (7,8) This review surveys the methods to determine the reinforcement parameters that play a very important role in controlling the performance of MMCs and the nondestructive test (NDT) methods which are used to detect the defects or monitor the defect evolution in MMCs.

3 Determination of reinforcement parameters

Methods to determine the reinforcement parameters are well reviewed in the literature. (5) In order to present this information as complete as possible, the methods collected in Ref. (5) are also included in the present review, but only shortly described. Several newly developed and interesting methods are presented in much more detail.

3.1 Aspect ratio

The aspect ratio plays a very important role in controlling the performance of MMCs, especially those containing short fibers or whiskers. For almost equiaxed particles, the aspect ratio can be measured on polished sections. For short fibers or whiskers, the simplest method of measurement is that described by Arsenault. (9) The reinforcement is brought into suspension by dissolving the matrix using a suitable acid. This is followed by sedimentation onto a glass or a metallic substrate upon which the fibers can be observed easily under a scanning electron or light optical microscope. Analysis can then be done either manually or by quantitative image analysis.

3.2 Reinforcement orientation

Properties of MMCs largely depend on the reinforcement alignment. A well aligned structure is generally anisotropic in properties (mechanical or electrical), whereas a randomly oriented structure is more isotropic. For potential commercial use, a microstructure with short fiber or whisker well aligned with the main stress axis is often preferred. Three methods for the assessment of the degree of alignment have been proposed.

- 1) Microscopical observation: (10-13) orientations of individual fibers are calculated on the basis of their elliptical intersection with a polished surface. D. Juul Jensen (10) and D. Van Hille (11) used this method to measure the orientations of SiC whisker and Al₂O₃ fibers in aluminum matrix, respectively. This method works well for large circular fibers of reasonable length, but is of dubious value for fine mis-sharpen short whiskers.
- 2) Fourier transform analysis: this is an elegant method, which involves the diffraction of light when passing through an optical micrograph. It requires many polished sections. However, it is difficult to separate and to quantify the influence of various factors. Chou (14) and Øvland (15) measured the whisker orientations in Al matrix following this approach.
- 3) Crystallographic analysis: in this method, texture information expressed as pole figures or orientation distribution functions is interpreted in terms of fiber alignment. Neutron or possible X-ray diffraction is used to determine the orientation distribution of the reinforcement, provided that the crystallographic orientation of the reinforcement can be related to its shape. D. Juul Jensen used this method to determine the orientation distribution of SiC whiskers in Al matrix. (10) However, this method is not appropriate for poorly aligned systems without a unique crystal direction.

3.3 Reinforcement distribution

Most research in the field of MMCs is focused on the development of methods to characterize the particle distribution. Particle clustering can be caused by insufficient mixing, sedimentation

or slow solidification rates. The constraints exerted by the elastic ceramic particles on the matrix alter the stress field in the vicinity of a cluster and give rise to local triaxial stresses which are much higher than the remote stress applied to the composite. ⁽¹⁶⁾ As a result, clusters can act as crack or decohesion nucleation sites or both at remote stresses which are lower than the matrix yield stress and which cause the MMCs to fail at unpredictable low stress levels. To improve the particle distribution in MMCs, reliable methods for identifying and quantifying such a distribution are very necessary.

A number of quantification methods have been developed, including the Dirichlet tessellation method, ⁽¹⁷⁾ the average interparticle spacing or mean free path, ⁽¹⁸⁾ the nearest and near neighbor distances, ⁽¹⁹⁾ the local area fraction, ⁽¹⁹⁾ the average number of particles contained within an imaginary test sphere of given size, ⁽²⁰⁾ the radial distribution function, ⁽²⁰⁾ the quadrat method ⁽²¹⁾ and local energy dispersive X-ray analysis techniques. ⁽²²⁾ In addition, a commercial software named *Tessellation Analysis Program* was recently developed at the Southampton University to quantify the spatial distribution of discrete objects in 2D images. Its measurements relating to the local neighborhood of every object are obtained by generating finite-body tessellations, which extend the Dirichlet/Voronoi tessellations (see Fig. 1(a)) for the quantification of the distribution of finite-size objects of different size, shape, orientation and/or area fraction. A finite-body tessellation consists of a network of cells that uniquely defines the area which is closest to the interface of the corresponding objects (Fig. 1(b)). It was developed by Boselli and co-workers, specifically to characterize high volume fractions of second phase particles of widely varying size and shape. ⁽²³⁾ This method has been shown to be more sensitive to local distribution characteristics than the original Dirichlet tessellations, as it avoids physically unrepresentative tessellation features such as a cell which is smaller than its associated particle. This can happen when particles with significantly different sizes are present in the microstructure. A trial version (30 days limitation) can be downloaded from the website <http://www.demon.co.uk/ffaltd/tapweb.html#download>.

Besides the method of finite body tessellation, other methods, such as intercept method, quadrat method and radial distribution function, were found to be also very effective in detecting pronounced changes in the MMC microstructure through appropriate parameters. ^(21,24) L. van Vugt and L. Froyen investigated the agglomeration of particles in Al-7%Si-15%SiC materials prepared by solidification in the Russian space station MIR and on earth. ⁽²⁴⁾ With their method, a low magnification technique is used in a quantitative image analysis system. As a consequence, individual SiC particles are neglected and zones with a significant number of particles are considered as single zones, and then its mean intercept length is measured. A high value of this mean intercept length indicates a high agglomeration degree. The results show that microgravity and high cooling rate decreases the agglomeration of the SiC particles.

With the quadrat method, ⁽²⁵⁾ the image to be studied is divided into a grid of square cells and the number of particles in each cell are counted. A schematic diagram is presented in Fig. 2(a). The principle is that the number of particles in each cell changes with the particle distribution. For example, an ordered particle distribution would be expected to generate a large number of quadrats containing approximately the same number of particles, however, a clustered distribution would lead to a combination of empty quadrats, quadrats with a small number of particles and quadrats with many particles. In this method, the major problem is determining the optimal quadrat size, which can be found by physical analysis of the microstructure.

Karnezis used this method to analyze the particle distribution in A356/10%SiC_p and A356/20%SiC_p materials processed by gravity casting, squeeze casting, and roll casting. ⁽²¹⁾ The quantitative results can be related to the properties of particulate MMC systems and provide an alternative method for understanding the factors that affect MMC behavior.

With the radial distribution function, ⁽²⁶⁾ a circular disc of radius r is centered on a particle and the number of particles in the disc is counted to determine the distribution function (Fig. 2(b)):

$$H(r) = \frac{N_{ra}}{N_a} \quad (1)$$

where N_{ra} is the mean number of particles per unit area in a circular disc of radius r and N_a is the mean number of particles per unit area over the whole sample. For a random distribution of particles, the $H(r)$ function has a constant value of 1. Karnezis and co-workers evaluated this method by measuring the particle distribution in A356/10%SiC_p and A356/20%SiC_p materials. ⁽²¹⁾

3.4 Density-Archimedean densitometry

The accurate measurement of the density of a sample can be used to evaluate the pore content. The measurement of the porosity level is possible within 0.5% (absolute value). On the other hand if the composite is completely densified, the reinforcement content can be evaluated ($\pm 1\%$, depending on the relative reinforcement/matrix densities). This is especially useful for spray formed composite material because the volume fraction of reinforcement actually incorporated into the composite is often unknown.

3.5 Fiber strength distribution

The tensile strength distribution of fibers is a key constitutive property of fiber reinforced composites and is often described using Weibull statistics. However, the standard experimental methods used for obtaining the Weibull parameters are tedious and prone to error. J. He et al. described a new method to determine the Weibull parameters of polycrystalline alpha-Al₂O₃ fibers (Nextel 610). ⁽²⁷⁾ With their method, the Weibull parameters of fibers are determined from piezospectroscopic measurements by using photo stimulated Cr³⁺ luminescence (fluorescence) during fiber bundle tests. The fiber bundle stress, the stress on the surviving fibers and the survival probability can be obtained by the deconvolution of the luminescence spectra. A qualitative method was developed to assess whether the fibers in a bundle are aligned by monitoring the broadening of luminescence linewidth as a function of the applied load.

4 Defects and non-destructive techniques

Defects and anomalies are generated unintentionally during two different situations: the manufacturing and the service life of the composite. Table I lists the possible defects in MMCs.

Table II lists some NDT techniques used for composites, including the advantages and the disadvantages for each technique. NDT can be performed prior to the final failure either in real time by continuously monitoring the composite during service or at selected service intervals by removing the composites from the load environment to perform the tests. The principal

objective is to provide the assurance on the quality and structural integrity of a particular component. As a general guide there are two main approaches of the use of NDT to assess quality. The first one aims to provide a qualitative assessment. The second one is less subjective and employs quantitative acceptance standards. Since NDT methods have different sensitivities to different types of damage, as a general rule, two or more NDT methods should be used to provide complementary information on the state of damage to composites. Techniques used are acoustic emission, ultrasonics, eddy currents, radiography, computed tomography, thermography, low frequency vibration and noncontacting electromagnetic acoustic transducers.

4.1 Acoustic emission

Acoustic emission (AE) is a term used to describe the resulting stress waves when strain energy is rapidly released due to microstructural changes in the material. When the stress waves reach the specimen surface the small displacements produced are detected by a transducer. The amplified signal is then conditioned, recorded and finally analyzed. The detected electrical signals are influenced by the aspects of the stress wave propagation: the geometric spreading, the losses due to material absorption, the direct and reflected paths from the acoustic emission source to the transducer, and the different speeds of the propagation of the stress waves together with the dispersion of the stress wave. AE offers the potential to monitor damage accumulation in real time, to distinguish between different micro-damaging mechanisms and to establish their spatial and temporal coordinates. However, its interpretation is difficult and is based on a correspondence between the AE characteristics of the signal and the different modes of failure that are known to occur in MMCs. Two interpretations were made on an amplitude basis and a frequency analysis. (28,29) AE is very sensitive to register incremental crack lengths in brittle materials with high crack velocities, but is rather insensitive to larger crack growth in very ductile materials with low crack velocities.

The amount of continuous emission detected is different for whisker and particulate composites. For example, a particulate SiC_p MMC showed a considerable continuous emission after yielding. (30) The whisker reinforced composite showed only an increase in burst emission during the test. The rate of emission increases with reinforcing particle size and volume fraction but is independent of matrix alloy composition (here the matrix is aluminum or aluminum alloys, which are often very ductile). (31,32) The peak amplitude distributions of the particulate composites are often narrow and of a low intensity level, whereas the whisker composites have a higher amplitude. In a whisker reinforced composite high amplitude events are assumed to be related to whisker fracture, while lower amplitude events are related to matrix inelastic deformation and whisker-matrix interfacial failure. (32) Fig. 3 summarizes the cumulative amplitude distribution of AE events for tensile tests of a single-crystal Al containing a single SiC fiber, which was prepared by two growth velocities, resulting in quite different interfacial microstructures. (33) The dashed lines denote the number of fractures observed after testing. For the rapidly solidified composite which has a higher bonding strength, most of the large amplitude AE events are below the dashed line, so there is a good correspondence between the number of large AE events and the number of fiber fractures actually observed. However, for the slowly solidified material, there are many more AE events exceeding the background level than can be accounted from the fiber fractures. These extra signals were caused by interface cracking because this material has a weaker interface.

The feasibility of using AE as an in-process, nondestructive quality control technique was examined during squeeze casting of Al alloy A356 reinforced with continuous alumina-silicate fibers. (34) The optimum location of the transducers and the frequency response of the ambient noise, preform crushing (here the preform is a rigid, porous, interconnected network of low cost alumina-silicate fibers with silica binder added for dimensional stability; preform crushing means that the preform is compressed and deforms if during the infiltration process the molten alloy solidifies prematurely near the cold die walls or the pressure required to infiltrate the preform is greater than its compressive strength) and metal solidification were identified using three transducers. The high frequency transducer was considered to be more sensitive to preform crushing and metal solidification. However, metal solidification could not be distinguished from the combined processes of infiltration-solidification, although gross preform crushing could be detected as a warning of incomplete infiltration based on the integrated signal intensity spectrum.

As another application, an AE technique has been developed to study the microstructural changes in Mg matrix composite containing Al₂O₃ (Saffil) short fibers which are submitted to thermal cycling. (35) A significant dependence of the AE activity (AE count per temperature unit) on T_{top} (T_{top} is maximum temperature during thermal cycling) was found during thermal cycling with a step by step increased T_{top}. At a constant T_{top} the AE count sums do not significantly depend on the number of cycles (up to 40 cycles). It is shown that the thermal stresses are accommodated by dislocation generation and motion in certain temperature ranges depending on the upper cycling temperature and the amount of reinforcement.

AE monitoring also allows the experimental measurement of the void nucleation response in a PRM as a function of strain. (31,36-39) An acoustic investigation during the bending test of Al6061 with 30% of 10 μm alumina particles shows that two types of AE events can be distinguished: (39) at very low strain level, void nucleation is the main source for AE; at higher levels the micro pop-in of primary voids and their eventual coalescence results in a different type of AE. The sensitivity of void detecting is related to the particle size. (39) For fine particle reinforced composites, it is difficult to detect the void nucleation at the interface between the fine particles and the matrix. The number of the detectable events increases during the void nucleation if the particle size increases. By measuring the AE signals, the nucleation velocity of micro-cracking (termed source velocity in ref. (39)) can be calculated. The source velocity has a higher value during the void nucleation but becomes low during the void coalescence.

The evaluation of the tensile damage in Al2014 alloy reinforced with a nominal volume fraction of 20% α-Al₂O₃ particulates indicates that AE monitoring is an appropriate method for accurate investigations of the reinforcement damage during loading. (40) Compared with the matrix material, a much higher number of AE events in MMC was due to particulate damage. (33) A similar phenomenon can be found in MFRM. (41) The characteristic AE with distinct waveforms was found for MMCs containing the different fibers (SCS-2 fiber produced by Textron and Σ fiber produced by Sigma, the former is a SiC fiber CVD deposited on a carbon filament core and has a surface carbon-rich layer while the latter has a tungsten core) during the tensile test (see Fig. 4). (41) The waveform characteristic of the *in situ* fracture of SCS-2 fibers contains at least two wave packets of relatively high intensity (Fig. 4(a)), whereas the waveform typical of the *in situ* fracture of the Σ fibers consists of a single damped wave packet of a shorter duration and a lower intensity (Fig. 4(b)). The reason is different ductility of the two fibers.

These waveforms, which are characteristic for the fiber fracture, are distinctively different from that accompanying matrix rupture (Fig. 4(c)).

AE can also be used for fatigue crack growth monitoring in MMCs. A. Niklas and co-workers investigated the AE behavior during fatigue propagation in aluminum 6061 and aluminum 6061 matrix composites containing 5, 10, and 20 wt.% SiC particle reinforcement under tension-tension fatigue loading. ⁽⁴²⁾ The cumulative number of AE events was found to correspond closely to that of the fatigue crack growth. The rates of AE events increased with increased crack propagation rate (see Fig. 5). The characteristics of the AEs detected during crack propagation were similar to those observed during tensile testing. Similar results were obtained in Ti-45Al-7.5TiB₂ under tension-tension and compression-compression loading. ⁽⁴³⁾ Another attractive application of AE in fatigue is that it can be used to predict the residual fatigue life. ⁽⁴⁴⁾ D. Shan and H. Nayeb-Hashemi investigated the tensile behavior of 6061-T6 aluminum alloy reinforced with 15% volume fraction SiC particulates with and without fatigue damage using the AE technique. ⁽⁴⁴⁾ They used a slow loading rate to increase the AE sensitivity and to prevent the AE event pile-up. The tensile tests of post fatigue specimens show that the number of cumulative events exponentially increases after material yielding and this increase slows down before the final failure. The initial exponential increase of the AE events is related to the numerous void nucleations at the particle-matrix interfaces. D. Shan and H. Nayeb-Hashemi defined a function to describe the probability of a particle debonding at an applied far field strain level, assuming that the variation of local strain and stress field at the particle-matrix interfaces with particle size, orientation and local volume fraction obeys a Weibull distribution. ⁽⁴⁴⁾ If one further assumes that the number of the AE events during the subsequent tensile tests is proportional to the number of particles debonded, then the cumulative events at an given applied strain can be calculated and the residual fatigue life of a specimen can be predicted by testing the post fatigue specimen in tension and monitoring the AE events. These model predictions well agree with the experimental data.

4.2 Scanning acoustic microscopy

Scanning acoustic microscopy uses a water-coupled lens to transmit a focused beam of high-frequency sound on the specimen. The contrast is produced from the acoustic energy which is reflected by the surface after first interacting with it to a depth of approximately one Rayleigh wavelength. The contrast obtained in scanning acoustic microscopy is directly related to the elastic properties of the surface. Therefore, an image can be obtained if different elastic properties coexist in the examined area. This allows the discrimination of optically transparent phases and the imaging of extremely fine surface cracks and pores via the mechanism of the Rayleigh-wave-fringe formation. Its resolution depends on the diameter of the acoustic beam and the focal convergence. The minimum detectable defect should be larger than or equal to one Rayleigh wavelength. It was reported that it was highly sensitive to the presence of cracks and elastic discontinuities in materials. ^(45,46)

Scanning acoustic microscopy has been used to study the progressive deterioration of the fiber-matrix interface in Ti-6Al-4V reinforced with silicon-carbide monofilaments. ⁽⁴⁷⁾ It was found that it has a high sensitivity to the radial microcracks that formed in the SiC monofilaments as a result of heat treatment. Furthermore, it can monitor the degradation of the carbon-rich layer at the fiber-matrix interface in more sensitive manner.

4.3 Ultrasonics

Ultrasound is usually transmitted and received with a transducer of fixed frequency in the range of 1 to 10 MHz. The method consists of directing a beam of ultrasonic energy into a specimen and then measuring either the energy transmitted through the specimen, or the energy reflected from a discontinuity or a defect in the specimen. The propagation of ultrasound in a composite is influenced by different material parameters such as stiffness, density and microstructural features. In addition, factors such as the condition of the surfaces, the frequency and type of incident ultrasound wave also affect its propagation. Pulse-echo and through-transmission are the two basic methods of ultrasonic testing. The pulse-echo method measures the energy reflected from discontinuities or defects in the material. The through-transmission method measures the energy which traverses the composite specimen. The main disadvantage of ultrasonic inspection is that it needs a coupling medium between transducer-structure and that for a thorough study scanings in X- and Y-direction are needed.

Ultrasonic velocities are primarily correlated with the volume fraction of the reinforcement. (48,49) Therefore, it can be used to predict the volume fraction of reinforcement in a nondestructive manner. M. L. Dunn and H. Ledbetter used the ultrasonic velocities to investigate the orientation distribution of short fibers in a transversely isotropic Al-SiC MMC. (50) Their results agree reasonably with those obtained from neutron diffraction pole figures. The attenuation and the backscattering behavior is primarily related to the volume fraction of the fibers and these relations can be used to predict the fiber distribution in the matrix. Ultrasonic analysis is also an efficient tool to investigate the elastic properties and to characterize the anisotropy of MMCs on the basis of the longitudinal and shear wave velocities. (49,51-53) It can be used to control the elastic homogeneity of the material: it allows the determination of the elastic moduli with a much better accuracy than conventional tensile methods, especially regarding the shear properties and the Poisson's ratios.

The ultrasonic evaluation is sensitive to fabrication abnormalities of MMCs. (54,55) P. K. Liaw and G. Mott et al. reported that the ultrasonic method can be used to identify the SiC_p clusters as small as 1 mm. (7,48,53) Both axial (the ultrasonic beam is directed normal to the billet surface and therefore is parallel to the billet axis) and circumferential (scanning is conducted around the circumference of the billet by rotating the billet) ultrasonic scanings detected the presence of SiC_p clusters in 335 mm long × 349 mm diameter MMC billets fabricated by powder metallurgy. (8) P. L. Blue performed ultrasonic inspection of silicon carbide whisker and particulate reinforced aluminum metal matrix composite billets, extrusion, forgings, and rolled plate and sheet. (56) His results revealed the presence of porosities and flaws.

Using ultrasound, the free edge effect can be assessed. (57-59) This is a stress concentration that exists at the lateral edge of laminates which are subjected to stress in the axial direction and which can lead to early failure of the laminate. It is caused by the transition in the stress state from the edge to the biaxial stresses within the interior of the laminate caused by the variation of Poisson's ratio from ply to ply. The transverse fiber/matrix interfacial failure and the fiber breakage associated with the fiber fragmentation process can also be investigated in MMCs. (57-59) S. F. Hu investigated the interfacial failure, the free edge effect and the fiber breakage in Ti-6Al-4V-SiC fiber (SCS-6) composite using the C-scan technique. (57) M. C. Waterbury and co-workers reported the use of non-destructive shear-wave back reflectivity ultrasound imaging with an *in situ* micro-straining stage to understand the process of fiber fragmentation in

titanium matrix composite. (58) A good agreement was found between the fiber breakages imaged by ultrasound and the breakages observed by metallography. However, if the fractures are too close to each other, interference can occur which makes the interpretation more difficult.

Fatigue damage can be assessed by *in-situ* ultrasonic monitoring of MMCs. By using the ultrasonic surface wave technique, in which the velocity and the attenuation coefficient of surface waves shows measurable variations with the number of fatigue cycles, the onset and extent of matrix cracking fatigue damage can be detected in titanium matrix composite (60) and in Al₂124-SiC_w materials (61). This method proved to be more sensitive to the accumulating damage than standard load-displacement modulus measurements.

Recently, special ultrasonic techniques have been used to detect the flaws in MMCs accurately. A new ultrasonic NDT technique using ultrasonic shear wave back reflectivity has been developed to characterize the interface between the fiber and the matrix in MMCs. (62,63) There are several advantages of using shear waves. First, shear waves have a shorter wavelength which leads to a higher resolution. Second, shear waves are more sensitive to interfacial failure due to the fact that the motion of the particle is in the transverse direction. D. J. Roth described a single transducer ultrasonic imaging method based on the ultrasonic velocity measurement that eliminates the effect of thickness variations. (64,65) This method uses a reflector located behind the sample and acquires echoes of the sample and reflector surfaces in two distinct scans. Fig. 6 shows the comparison of the imaging results for a MMC panel with different fiber volume fraction variations and a 12% edge-to-edge thickness gradient. (64) It was found that the thickness-independent ultrasonic images reveal and quantify correctly the areas of the microstructure variation within an accuracy of 1-2%. Its use can result in significant cost savings because the ultrasonic image can be interpreted correctly without the need to machine the specimens to achieve a precise thickness uniformity.

4.4 Noncontacting electromagnetic acoustic transducers (EMATs)

EMATs are used to generate and receive the ultrasonic signals. They permit ultrasonic measurements in air without the use of any acoustic coupling medium between the transducer and the component. This facilitates the scanning of the transducers over the surface of the structure. By using appropriately designed coils and magnetic field orientations, EMATs can be constructed to generate and to receive the desired symmetric lamb (SL) or shear horizontal (SH) waves. Both attenuation and velocity are measured for these propagation modes to permit the evaluation of structural variations, flaws and elastic constants. High precision velocity and attenuation measurements were used to locate defects and to determine the elastic moduli of graphite/aluminum (Gr/Al) plates and a tube. (66) Four transducers scanned the surface with an arrangement of two receivers located between two transmitters. The transmitter EMATs were excited with unipolar pulse (250A, 1 μs wide) at a 1 kHz repetition rate. The data show that the SL wave velocity and attenuation measurements can be used to evaluate the local variation in the properties of a plate. The SL and SH wave velocity data can be used in the determination of the in-plane elastic property. The resolution depends on the gage length between the two receiver transducers.

4.5 Eddy current technique

If a current-carrying coil is placed adjacent to a conducting material, eddy currents are induced into the material affecting the impedance of the driving coil. Local changes in resistivity or the interruption of the eddy-current field by defects will further alter the impedance. This response is usually characterized in terms of both the amplitude and the phase angle. These values will depend on the probe parameters, the material conductivity, the thickness and the defect dimensions. The spatial response of the probe, i.e. its sensitivity to a given size of defect, depends on both the geometry of the coil and the driving frequency. A critical factor is the selection of this frequency.

Since the eddy current response of the MMCs is dependent on the material density and the volume fraction of the reinforcement, it has been developed to determine the reinforcement volume fraction of MMCs. (7,52,67) It combines a micromechanical concept with the measurement of the anisotropic electrical conductivity. When the measured conductivity is coupled with the theoretically predicted conductivity, the unknown reinforcement volume fraction can be calculated. This technique is also effective to detect near-surface density variations as it is sensitive to surface irregularities, (7,8,48,68) to identify the matrix powder alloy chemistry and particle size (52) and to estimate the total volume percentage of reinforcement and intermetallic compound formed during the processing stage. (48,67)

4.6 Radiography

A variety of penetrating particles and rays, including neutron, gamma and x-rays, are used to study composites based on their different absorption in passing through a material. Because of the variations in thickness or the differences in absorption characteristics caused by variations in compositions, different parts of a component absorb different amounts of radiation. Unabsorbed radiation passing through the component may be recorded on film, viewed on a fluorescent screen or monitored by a radiation detector.

X-ray radiography can reflect the density of Al-SiC composites. (69) It has been used to investigate imperfections such as fiber breakages and voids in Ti-6Al-4V containing boron fiber coated with BC. (68) It is also useful to analyze fiber displacement, orientation and fiber swimming. (54) Fiber swimming is a term used to refer to a location where several fibers have noticeably deviated from the desired orientation .

4.7 Computed tomography (CT)

A computer assisted tomographic scanner operates by combining the power of a computer with traditional radiography techniques. Flaws are detected by rotating the object relative to a radiation source and a set of detectors. The source consists of either a gamma ray emitting isotope, such as iridium 192 or cobalt 60, or a high intensity X-ray tube. The detectors collect transmission data from the object at a number of different angles. The information is transformed by the computer into a two-dimensional density map of the desired cross section. By taking multiple scans of the object a three dimensional picture can be synthesized with a computer. Defects as small as 25 μm can be resolved with the present microfocus X-ray tubes.

The CT can detect the heterogeneous distribution of particles and porosities at a mesoscopic scale, but not isolated ones in a cast MMC. (70) The inspection of fiber FP (fiber FP is a

continuous polycrystalline alumina fiber) reinforced MMCs showed that this technique is very useful to detect porosity and delaminations and to characterize complex components containing varying thickness and curved surfaces. ⁽⁵⁵⁾ It offers advantages over traditional radiography as it takes individual slice planes from multiple directions making it possible to not only locate the defect positions but also to characterize the defect size. High resolution X-ray computed tomography can detect the particle cracks and the matrix cracks with an opening of less than 1 μm in MMCs thanks to the phase contrast technique. ⁽⁷¹⁾ Fig. 7 gives a tomographic image of the Al6061-12% SiC_p with a particle size of 120 μm submitted to the tensile deformation.

4.8 Thermography

When a uniform heat flux is applied to the surface of a composite structure, the heat flow pattern through the structure is altered by defects that may be present and thus produce local temperature differences on the surface of the structure. Thermography is the mapping of the resulting surface temperature. An infrared sensitive camera can be used to record the temperature distribution and the output stored on videotape. The sensitivity of thermography is strongly dependent on thermal conductivity of the inspected material and on the effect of the individual type of defect on this property.

Very little work has been done to characterize the defects in MMCs using this technique. The inspection of Ti-6Al-4V containing boron fiber coated with BC proved to be inconclusive because the material has a very high thermal conductivity. ⁽⁶⁸⁾

4.9 Low frequency vibration

Low frequency vibration methods are split into two categories: 'global' methods, which involve measurement of the natural frequencies and/or damping of the whole component and 'local' methods in which a vibration property of the region of the structure around the test point is measured. Global methods offer the possibility of very rapid testing, but unfortunately they are not very sensitive.

One interesting use of this method is to evaluate the damage in MMCs with the measurement of the longitudinal Young's modulus, which is related to the measured frequency. Y. Dorgeuille and co-workers investigated the damage evolution in a Ti-6Al-4V-35% SiC fibers during the thermal cycling using this method. ⁽⁷²⁾ They found that a sudden decrease in the longitudinal Young's modulus corresponds to a point where the failure stress drops dramatically. They further managed to correlate decohesion with the decrease in the longitudinal Young's modulus, thus demonstrating the possibility to evaluate the damage.

5 Summary

The methods to determine the reinforcement parameters and the NDTs to monitor or evaluate the defects in MMCs have been reviewed. The reinforcement parameters, including the aspect ratio, orientation, distribution and density, can well be determined by the suggested methods. However, the methods developed to determine the reinforcement orientation are time-consuming or expensive or not portable. New methods, with low cost, convenient use and high precision should be developed. Acoustic emission, ultrasonics, eddy current and computed tomography methods have extensively been used to evaluate the defects in MMCs. The EMATs, radiography, thermography and low frequency vibration methods have not been employed

extensively because of their high cost and/or unsuitability. AE methods have been proved to be effective tools to control quality during the fabrication of MMCs, to investigate the microstructural change during the thermal cycling, to monitor the void formation and the reinforcement damage during loading and to study the crack growth during fatigue. Ultrasonics methods are suitable for obtaining the reinforcement parameters and are an efficient tool for investigating the elastic properties. They are also sensitive to abnormalities in MMCs and therefore can be used to detect the defects, such as the particle clustering and porosity, produced during fabrication, and to investigate the interfacial failure and the fiber breakage during loading. Eddy current is a promising method to determine the volume fraction of the reinforcement in MMCs with high efficiency and convenience. The attractive characteristic of computed tomography is that this technique can not only locate the defect but also characterize the defect size.

As a final comment it should be pointed out that the resolutions and the sensitivities of the used NDTs in MMCs were marginally emphasized in the past research works, although several papers focused on developing the mechanics tools necessary to establish the flaw criticality from the NDT measurements. Very little has been published on mathematical models which predict the mechanical response of a MMC containing manufacturing or service-induced damage. Therefore, validation of NDT techniques, life-time prediction tools and relationship between NDT results and component performance should be particularly emphasized in future research and R&D efforts.

6 Acknowledgement

This work was supported by a website project from the European Commission: assessment of metal matrix composites (MMC-Assess), under the contract no. ERB BRRT-CT98-5061. The homepage is <http://mmc-assess.tuwien.ac.at/>. The authors would like to thank Dr. Frédéric Charlot and Dr. Paul Wambua for their helpful discussions.

Figure captions

- Fig. 1.** (a) Dirichlet tessellation, which is simply a network of polygons generated around the particles such that all points within a polygon lie closer to the center of the enclosed particle than to any other; (b) finite-body tessellation. (23)
- Fig. 2.** (a) Schematic representation of the quadrat method, using four quadrats. Counted particles are denoted in black; (21) (b) schematic representation of the method used to determine the radial distribution function. Particles identified as disc centers are denoted in grey and counted particles in black. The outer frame size is 760×510 pixels, the disc has a radius r , and all dimensions are in pixels. (21)
- Fig. 3.** Cumulative amplitude distribution of AE events (rms volts) for tensile tests. Each curve is the average of two tests. The straight line boundary marking the shaded portion of each curve represents the average number of fiber fractures determined by dissolving the matrix in a solution of warm sodium hydroxide. The number of fractures is also indicated by the arrow from each curve label. (33)
- Fig. 4.** AE waveforms typical of: (a) in situ fiber fracture of Al6061/SCS-2; (b) in situ fiber fracture in Al6061/ Σ samples and (c) matrix rupture. (41)
- Fig. 5.** Number of AEs per load cycle vs crack propagation per load cycle for Al 6061 containing 5, 10, and 20 wt.% SiC particles. (42)
- Fig. 6.** Ultrasonic images of MMC panel having fiber volume fraction variation and a 300 μm thickness gradient edge-to-edge (lengthwise). (a) C-scan peak amplitude image where back wall echo was gated, 10 MHz. (b) C-scan peak amplitude image where back wall echo was gated, 30 MHz. (c) apparent velocity image, 10 MHz. (d) thickness-independent velocity image, 10 MHz. (64)
- Fig. 7.** Tomographic images of the composite showing the shape of two matrix cracks (arrow A and B) within the sample. (71)

Table I Defects in Composites

<i>Manufacturing type of defects</i>	<i>In-service type of defects</i>
Density; fiber ratio; porosity; delaminations; contamination; interface quality; thermal cracking; fiber alignment; foreign inclusions; fiber cuts; bonding defects	Impact damage; chemical/physical degradation; moisture pickup; static/dynamic overloading; corrosion attack; heat influence

Table II NDT Techniques Used for the Composites

Methods	Typical defects detectable	Reliability	6.1.1 Sensitivity	Speed	Convenience	Cost
Conventional ultrasonic	Delaminations; porosity; cracks; inclusions; fiber distribution; fiber alignment; curing state	Good if automate	Very good for delaminations, inclusions, voids, porosity	Relatively slow: point to point test	Poor-need for couplant	Low if manual testing, high if automate
X-radiography	Inclusions; fiber alignment; fiber distribution; cracks; voids	Good	Good for inclusions, translaminar	Good	Poor-need for screening etc	Modest for basic system, high for more flexible systems
Thermography	Delaminations; fiber concentrations; bonding defects; inclusions	Good provided heat source suitable and images obtained over suitable time range	Moderate for delaminations and inclusions; not applicable to other defects	Good	Fair	High
Low frequency methods	Incorrect fiber volume fraction; cracks; large delaminations; incorrect winding angle	Relatively low	Poor only useful for relatively large delaminations	Slow for large area coverage	Good-portable equipment; suitable for field use	Low
Laser ultrasonic	Delaminations; interface cracks; inclusions; fiber alignment	Good	Good	Fairly good	Fair	Very high
Shearography	Only delaminations; inclusions	Good provided excitation satisfactory	Moderate for delaminations and inclusions; not applicable to other defects	Good	Fair	High
Eddy current	Laminate composition; cracks	Good	Suitable for checking of volume fraction of reinforcement	Good	Simple to use and no contact with specimens	Low
Acoustic	Cracks; delamination;	Good provided that a	Good for detection of	Good	Good, easy to	Low

emission	damage propagation	correspondence between the AE characteristics of the signal and the different modes of failure was well setup	damage accumulation within bulk specimens		undertake, restrictions on specimen size and shape	
-----------------	--------------------	---	---	--	--	--

References:

1. S. Suresh, A. Mortensen, and A. Needleman, *Fundamentals of Metal Matrix Composites*, Butterworth-Heinemann, Stoneham, USA, 1993.
2. K. U. Kainer, *Metallische Verbundwerkstoffe*, DGM Verlag, Oberusel, Germany, 1994.
3. W. S. Johnson, *Metal Matrix Composites-Testing, Analysis and Failure*, ASTM, Philadelphia, USA, 1989.
4. S. A. Gieskes, and M. Terpstra, *Metal Matrix Composites, A Study of Patents and Patent Application and Other Literature*, Elsevier Science, New York, USA, 1991.
5. T. W. Clyne, and P. J. Withers, *An Introduction to Metal Matrix Composites*, Cambridge University Press, Cambridge, 1993.
6. P. Prader et al., "Internet Homepage of MMC-Assess", <http://mmc-assess.tuwien.ac.at/>, TU-Wien.
7. P. K. Liaw, R. E. Shannon, W. G. Clark Jr., W. C. Harrigan Jr., H. Jeong, and D. K. Hsu, "Determining Material Properties of Metal-Matrix Composites by NDE", *JOM*, **44**, 36-40 (1992).
8. R. E. Shannon, P. K. Liaw, and W. C. Harrigan Jr., "Nondestructive Evaluation for Large-Scale Metal-Matrix Composite Billet Processing", *Metall. Trans. A*, **23A**, 1541-1549 (1992).
9. R. J. Arsenault, "The Strengthening of Al Alloy 6061 by Fiber and Plated SiC", *Mater. Sci. Eng.*, **64**, 171-181 (1984).
10. D. Juul Jensen, H. Lilholt, and P. J. Withers, "Determination of Fiber Orientations in Composites With Short Fibers", in *Mech. & Phys. Behav. of Met. and Ceramic Mat. Composites, Proc. of 9th Risø Symp.*, S. I. Andersen, H. Lilholt, and O. B. Pedersen, eds., 1988, Risø National Laboratory, p. 413-420.
11. D. Van Hille, S. Bengtsson, and R. Warren, "Quantitative Metallographic Study of Fiber Morphology in a Short Fiber Al₂O₃ Fiber Reinforced Al Alloy Matrix", *Comp. Sci. Tech.*, **35**, 195-206 (1989).
12. D. Hull, *An Introduction to Composite Materials*, Cambridge Univ. Press, Cambridge, 1981.
13. M. Vincent, and J. F. Agassant, "Experimental Study and Calculation of Short Glass Fiber Orientation in a Center Gated Molded Disc", *Polymer Comp.*, **7**, 76-83 (1986).
14. T. W. Chou, R. L. McCullough, and R. Byron Pipes, "Composites", *Sci. Am.*, **255**, 166-177 (1986).
15. S. Øvland, and K. Kristiansen, "Characterization of Homogeneity and Isotropy of Composites by Optical Diffraction and Imaging", in *Mech. & Phys. Behav. of Met. and Ceramic Mat. Composites, Proc. of 9th Risø Symp.*, S. I. Andersen, H. Lilholt, and O. B. Pedersen, eds., 1988, Risø National Laboratory, p. 527-532.
16. D. J. Lloyd, "Aspect of Fracture in Particulate Reinforced Metal Matrix Composites", *Acta Metall. Mater.*, **39**, 59-71 (1991).
17. J. J. Lewandowski, C. Liu, and W. H. Hunt, "Effects of Matrix Microstructure and Particle Distribution on Fracture of an Aluminum Metal Composite", *Mater. Sci. Eng.*, **A107**, 241-255 (1989).
18. I. C. Stone, and P. Tsakirooulos, "Characterization of Spatial Distribution of Reinforcement in Powder Metallurgy Route Al/SiC_p Metal Matrix Composites 1: Techniques Based on Microstructure", *Mater. Sci. Tech.*, **11**, 213-221 (1995).
19. W. A. Spitzig, J. F. Kelly, and O. Richmond, "Quantitative Characterization of Second Phase Populations", *Metallog.*, **18**, 235-261 (1985).
20. K. H. Hanisch, and D. Stoyan, "Stereological Estimation of the Radial Distribution Function of Centers of Spheres", *J. Microsc.*, **122**, 131-141 (1981).
21. P. A. Karnezis, G. Durrant, and B. Cantor, "Characterization of Reinforcement Distribution in Cast Al-Alloy/SiC_p Composites", *Materials Characterization*, **40**, 97-109 (1998).

22. I. C. Stone, and P. Tsakirooulos, "Characterization of Spatial Distribution of Reinforcement in Powder Metallurgy Route Al/SiC_p Metal Matrix Composites 2: Techniques Based on Local Energy Dispersive X-ray Analysis", *Mater. Sci. Tech.*, **11**, 222-227 (1995).
23. J. Boselli, P. D. Pitcher, P. J. Gregson, and I. Sinclair, "Secondary Phase Distribution Analysis Via Finite Body Tessellation", *J. Microscopy*, **195**, 104-112 (1999).
24. L. van Vugt, and L. Froyen, "Gravity and Temperature Effects on Particle Distribution in Al-Si/SiC Composites", *J. Mater. Proc. Technol.*, **104**, 133-144 (2000).
25. A. Rogers, *Statistical Analysis of Spatial Dispersions: The Quadrat Method*, Pion, London, 1974.
26. B. D. Ripley, "Modeling Spatial Patterns", *J. R. Stat. Soc.*, **B39**, 172-191 (1977).
27. J. He, and D. R. Clarke, "Determination of Fiber Strength Distributions From Bundle Tests Using Optical Luminescence Spectroscopy", *Proceedings of the Royal Soc. London, Series A, Mathematica. Phys.*, **453**, 1881-1901 (1997).
28. J. Awerbuch, and J. G. Bakuckaus, "On the Applicability of Acoustic Emission for Monitoring Damage Progression in MMCs", in *Metal Matrix Composites: Testing, Analysis and Failure Modes*, W. S. Johnson, eds., 1989, ASTM STP 1032, Philadelphia, p. 68-99.
29. S. De Bondt, L. Froyen, and A. Deruyttere, "Monitoring Failure Processes in Unidirectional Al-SiC Composite by AE", in *Mech. & Phys. Behav. of Met. & Ceramic Mat. Composites, 9th Risø Symp.*, S. I. Andersen, H. Lilholt, and O. B. Pedersen, eds., 1988, Risø National Laboratory, p. 339-343.
30. C. Johnson, K. Ono, and D. Chellman, "Acoustic Emission Behavior of MMCs", in *2nd Int. Conf. on AE*, eds., 1985, Nevada USA, p. S263-S268.
31. P. M. Mummery, B. Derby, and C. B. Scruby, "Acoustic Emission From Particulate-Reinforcement Metal Matrix Composite", *Acta Metall. Mater.*, **41**, 1431-1445 (1993).
32. J. Awerbuch, J. Goering, and K. Buesking, "Minimechanics Analysis and Testing of Short Fiber Composites: Experimental Methods and Results", in *Testing Tech. of MMCs*, P. R. DiGiovanni, and N. R. Adsit, eds., 1988, Philadelphia, p. 121-142.
33. R. B. Clough, F. S. Biancaniello, H. N. G. Wadley, and U. R. Kattner, "Fiber and Interface Fracture in Single-Crystal Aluminum/SiC Fiber Composites", *Metall. Trans. A*, **21A**, 2747-2757 (1990).
34. S. Canumalla, R. N. Pangborn, B. R. Tittmann, and J. C. Conway Jr., "Acoustic Emission For In Situ Monitoring in Metal-Matrix Composite Processing", *Comp. Sci. Tech.*, **52**, 607-614 (1994).
35. F. Chmelik, Z. Trojanova, J. Kiehn, P. Lukac, and K. U. Kainer, "Non-Destructive Characterization of Microstructure Evolution in Mg Based Metal Matrix Composites Submitted to Thermal Cycling", *Mater. Sci. Eng.*, **234**, 774-777 (1997).
36. B. Y. Zhou, C. W. Lawrence, and B. Derby, "Acoustic Emission From A SiC Reinforced Al-2618 Metal Matrix Composite During Straining", *Scripta Mater.*, **37**, 1045-1052 (1997).
37. K. Komai, K. Minoshima, and H. Ryoson, "Tensile and Fatigue Fracture Behavior and Water-Environment Effects in a SiC-Whisker/7075-Aluminum Composite", *Comp. Sci. Tech.*, **46**, 59-66 (1993).
38. A. Rabiei, B.-N. Kim, M. Enoki, and T. Kishi, "Fracture Behavior in 6061 Al Alloy Matrix Composites With Different Reinforcements", *Mater. Trans. JIM*, **37**, 1148-1155 (1996).
39. A. Rabiei, M. Enoki, and T. Kishi, "A Study on Fracture Behavior of Particle Reinforced Metal Matrix Composites by Using Acoustic Emission Source Characterization", *Mater. Sci. Eng.*, **A293**, 81-87 (2000).
40. E. Gariboldi, C. Santulli, F. Sitavali, and M. Vedani, "Evaluation of Tensile Damage in Particulate-Reinforced MMC's by Acoustic Emission", *Scripta Mater.*, **35**, 273-277 (1996).
41. I. Roman, and R. Aharonov, "Mechanical Interrogation of Interfaces in Monofilament Model Composites of Continuous SiC Fiber-Aluminum Matrix", *Acta Metall. Mater.*, **40**, 477-485 (1992).

42. A. Niklas, L. Froyen, M. Wevers, and L. Delaey, "Acoustic Emission During Fatigue Crack Growth in SiC Particle Reinforced Al Matrix Composites", *Metall. Trans.*, **26A**, 3183-3189 (1995).
43. E. U. Lee, D. M. Granata, and W. R. Scott, "Acoustic Emission Monitoring of Fatigue in Titanium Aluminide XD Composite", in *Cyclic Deformation, Fracture, and Nondestructive Evaluation of Advanced Materials, ASTM STP 1157*, M. R. Mitchell, and O. Buck, eds., 1992, American Society for Testing and Materials, Philadelphia, p. 293-311.
44. D. Shan, and H. Nayeb Hashemi, "Fatigue Life Prediction of SiC Aluminum Composite Using a Weibull Model", *NDT Inter.*, **32**, 265-274 (1999).
45. C. W. Lawrence, G. A. D. Briggs, C. B. Scruby, and J. R. R. Davies, "Acoustic Microscopy of Ceramic-Fiber Composites: Part I Glass-Matrix Composites", *J. Mater. Sci.*, **28**, 3635-3644 (1993).
46. A. F. Fagan, G. A. D. Briggs, J. T. Czernuszka, and C. B. Scruby, "Microstructural Observation of Two Deformed Partially Stabilized Zirconia Ceramics Using Acoustic Microscopy", *J. Mater. Sci.*, **27**, 1202-1206 (1992).
47. C. W. Lawrence, G. A. D. Briggs, and C. B. Scruby, "Acoustic Microscopy of Ceramic-Fiber Composites: Part III Metal-Matrix Composites", *J. Mater. Sci.*, **28**, 3653-3660 (1993).
48. P. K. Liaw, R. E. Shannon, W. G. Clark Jr., and W. C. Harrigan Jr., "Nondestructive Characterization for Metal Matrix Composite Fabrication", in *Cyclic Deformation, Fracture, and Nondestructive Evaluation of Advanced Materials, ASTM STP 1157*, M. R. Mitchell, and O. Buck, eds., 1992, American Society for Testing and Materials, Philadelphia, p. 251-277.
49. J. H. Lee, and Y. C. Park, "Nondestructive Characterization of Metal Matrix Composite by Ultrasonic Measurement", *Composites Eng.*, **5**, 1423-1431 (1995).
50. M. L. Dunn, and H. Ledbetter, "Estimation of the Orientation Distribution of Short-Fiber Composites Using Ultrasonic Velocities", *J. Acoustical Soc. America*, **99**, 283-291 (1996).
51. D. Ducret, R. E. Guerjouna, P. Guy, M. R. Mili, J. C. Baboux, and P. Merle, "Characterization of Anisotropic Elastic Constants of Continuous Alumina Fiber Reinforced Aluminum Matrix Composite Processed by Medium Pressure Infiltration", *Composite Part A*, **31**, 45-55 (2000).
52. P. K. Liaw, R. E. Shannon, W. G. Clark Jr., W. C. Harrigan Jr., H. Jeong, and D. K. Hsu, "Nondestructive Characterization of Material Properties of Metal-Matrix Composites", *Mater. Chem. Phys.*, **39**, 220-228 (1995).
53. G. Mott, and P. K. Liaw, "Correlation of Mechanical and Ultrasonic Properties of Al-SiC Metal-Matrix Composite", *Metall. Trans. A*, **19A**, 2233-2246 (1988).
54. D. A. Stubbs, S. M. Russ, and P. T. MacLellan, "Examination of the Correlation Between NDE-Detected Manufacturing Abnormalities in MMCs and Ultimate Tensile Strength or Thermomechanical Fatigue Life", in *Cyclic Deformation, Fracture, and Non-destructive Evaluation of Advanced Materials: Second volume, ASTM STP 1184*, M. R. Mitchell, and O. Buck, eds., 1994, American Society for Testing and Materials, Philadelphia, p. 315-334.
55. J. E. Widrig, D. D. McCabe, and R. L. Conner, "Nondestructive Evaluation of Fiber FP Reinforced Metal Matrix Composites", in *Testing Technology of Metal Matrix Composites*, P. R. DiGiovanni, and N. R. Adsit, eds., 1988, American Society for Testing and Materials, Philadelphia, p. 227-247.
56. P. L. Blue, "Ultrasonic Inspection of Silicon Carbide Reinforced Aluminum Metal Matrix Composite Billets and Secondary Fabricated Products", in *Testing Technology of Metal Matrix Composites, ASTM STP 964*, P. R. DiGiovanni, and N. R. Adsit, eds., 1988, American Society for Testing and Materials, Philadelphia, p. 376-382.
57. S. F. Hu, "The Recent Development of an Ultrasonic Nondestructive Evaluation Technique for Metal Matrix Composites", *J. Composites Tech. Res.*, **19**, 41-44 (1997).

58. M. C. Waterbury, P. Karpur, T. E. Matikas, S. Krishnamurthy, and D. B. Miracle, "In Situ Observation of the Single-Fiber Fragmentation Process in Metal-Matrix Composites by Ultrasonic Imaging", *Comp. Sci. Tech.*, **52**, 261-266 (1994).
59. P. Karpur, T. Matikas, S. Krishnamurthy, and N. A. Ashbaugh, "Ultrasonic for Fiber Fragmentation Size Determination to Characterize Load Transfer Behavior of Matrix-Fiber Interface in Metal Matrix Composites", in *Proceedings, Review of Progress in Quantitative NDE*, D. O. Thompson, and D. E. Chimenti, eds., 1992, Plenum Press, New York, La Jolla, CA.
60. P. T. MacLellan, D. A. Stubbs, and P. Karpur, "In-situ Ultrasonic Surface Wave Assessment of Mechanical Fatigue Damage Accumulation in Metal Matrix Composites", *Composites Engineering*, **5**, 1413-1422 (1995).
61. J. D. Achenbach, M. E. Fine, I. Komsky, and S. McGuire, "Ultrasonic Wave Technique to Assess Cyclic-Load Fatigue Damage in Silicon-Carbide Whisker Reinforced 2124 Aluminum Alloy Composite", in *Cyclic Deformation, Fracture, and Nondestructive Evaluation of Advanced Materials, ASTM STP 1157*, M. R. Mitchell, and O. Buck, eds., 1992, American Society for Testing and Materials, Philadelphia, p. 241-250.
62. T. E. Matikas, and P. Karpur, "Ultrasonic Reflectivity Technique for the Characterization of Fiber-Matrix Interface in Metal Matrix Composite", *J. Appl. Phys.*, **74**, 228-236 (1993).
63. S. F. Hu, "The Transverse Failure of a Single-Fiber Metal Matrix Composite: Experiment and Modeling", *Composites Sci. Tech.*, **56**, 667-676 (1996).
64. D. J. Roth, "Using a Single Transducer Ultrasonic Imaging Method to Eliminate the Effect of Thickness Variation in the Images of Ceramic and Composite Plates", *J. Nondestructive Evaluation*, **16**, 101-120 (1997).
65. D. J. Roth, D. V. Carney, G. Y. Baaklini, J. R. Bodis, and R. W. Rauser, "A Novel Ultrasonic Method for Characterizing Microstructural Gradients in Tubular Structures", *Mater. Eval.*, **56**, 1053-1061 (1998).
66. R. W. Reed, "Noncontact Ultrasonic Evaluation of Metal Matrix Composite Plates and Tubes", in *Testing Technology of Metal Matrix Composites, ASTM STP 964*, P. R. DiGiovanni, and N. R. Adsit, eds., 1988, American Society for Testing and Materials, Philadelphia, p. 216-226.
67. H. Jeong, "Microstructure Modeling and Eddy Current Determination of Constituent Volume Fractions in Metal Matrix Composite", *Mater. Evaluation*, **55**, 1267-1273 (1997).
68. J. C. Duke, J. A. Govada, and A. Lemascon, "Nondestructive Evaluation of Boron-Carbide-Coated, Boron-Fiber-Reinforced Titanium", in *Mechanical Behavior of Metal-Matrix Composites*, J. E. Hack, and M. F. Amateau, eds., 1982, Composite Materials Committee of The Metallurgical Society of AIME and the Materials Science Division of American Society for Metals, Dallas, Texas, p. 259-282.
69. W. G. Clark Jr., and J. N. Iyer, "Structure Modeling and the Nondestructive Evaluation of Metal-Matrix Composites", *Mater. Eval.*, **47**, 460-465 (1989).
70. M. Gonazalez, G. Dominguez, and C. Bathias, "Some Results From Xray Computed Tomography Applied to Metal Matrix Composites", *J. Composites Tech. Res.*, **22**, 45-48 (2000).
71. J. Y. Buffiere, E. Maire, C. Verdu, P. Cloetens, M. Pateyron, G. Peix, and J. Baruchel, "Damage Assessment in an Al/SiC Composite During Monotonic Tensile Tests Using Synchrotron X-Ray Microtomography", *Mater. Sci. Eng.*, **234**, 633-635 (1997).
72. Y. Dorgeuille, P. E. Louvigne, and J. M. Lefeuvre, "Natural Frequency Method for a Quantitative Measurement of Damage Evolution in a Ti-6Al-4V/SiC Composite", *Composite Part B*, **29**, 451-458 (1998).

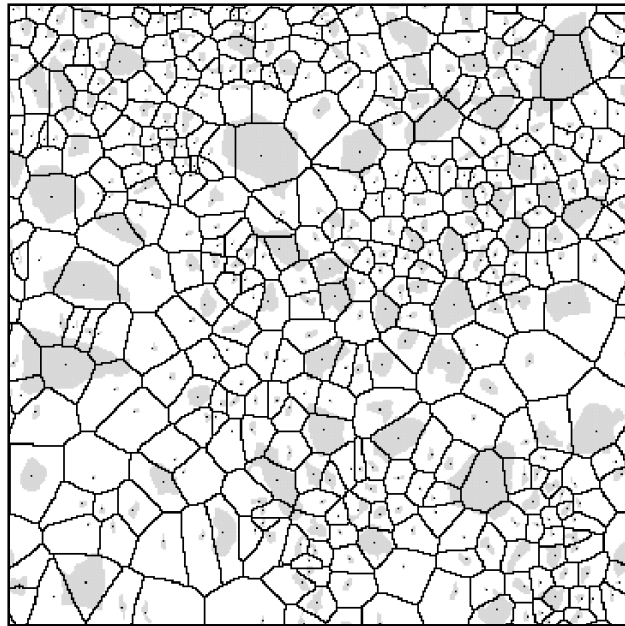


Fig. 1(a)

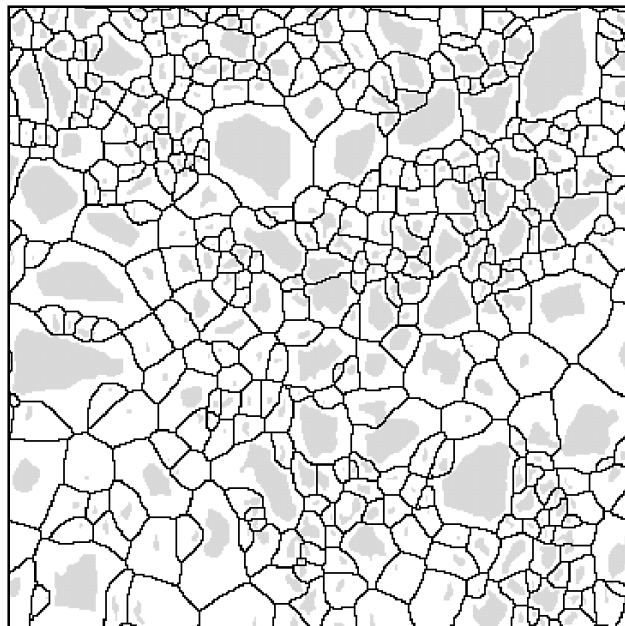


Fig. 1(b)

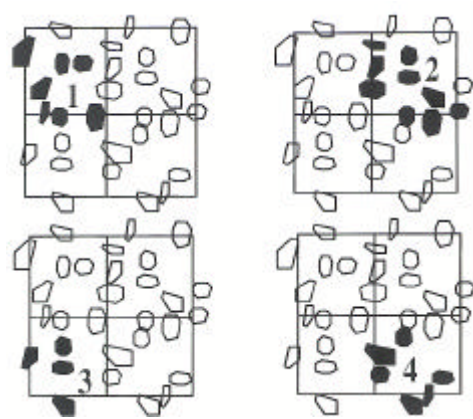


Fig. 2(a)

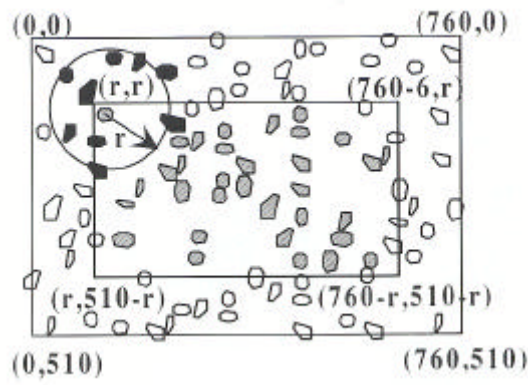


Fig. 2(b)

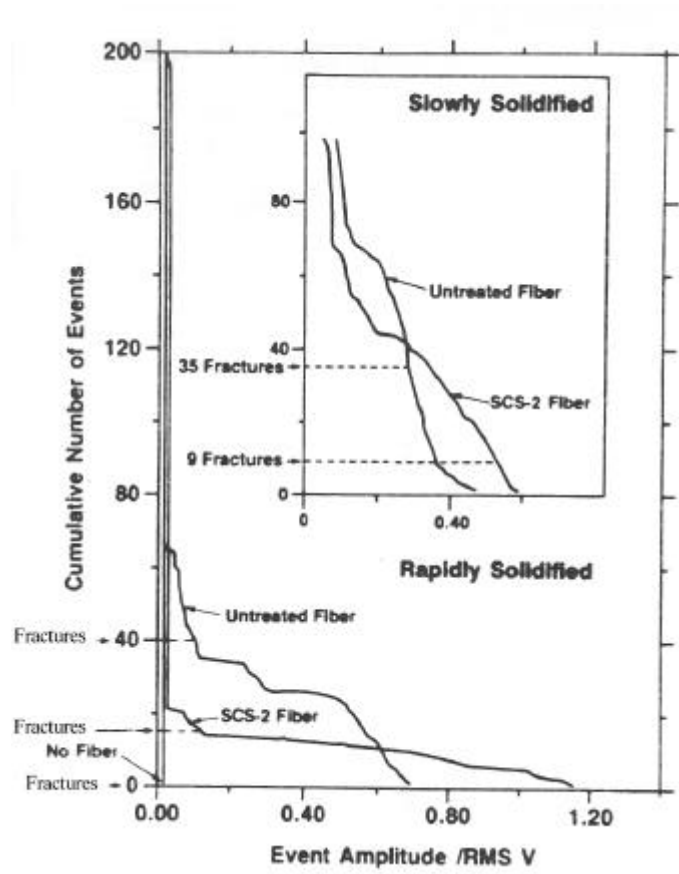


Fig. 3

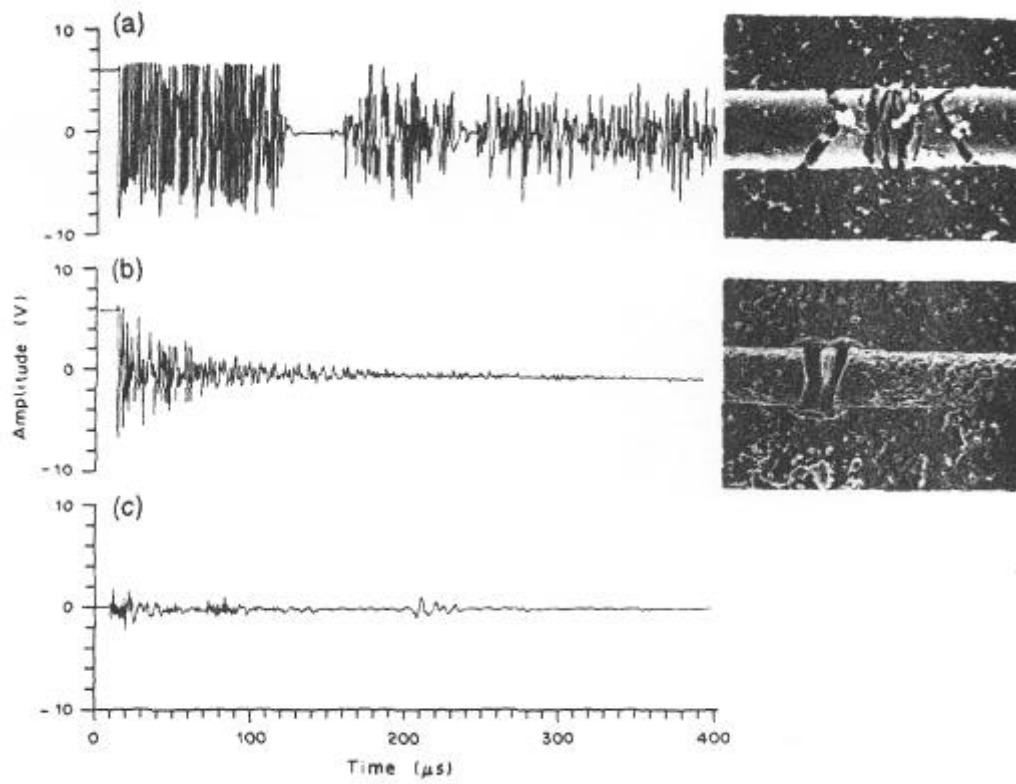
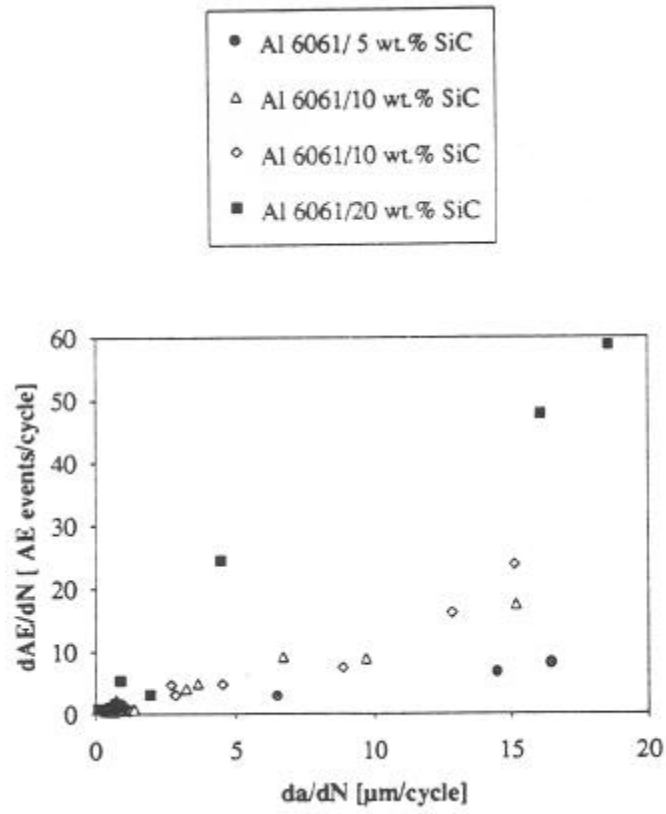


Fig. 4



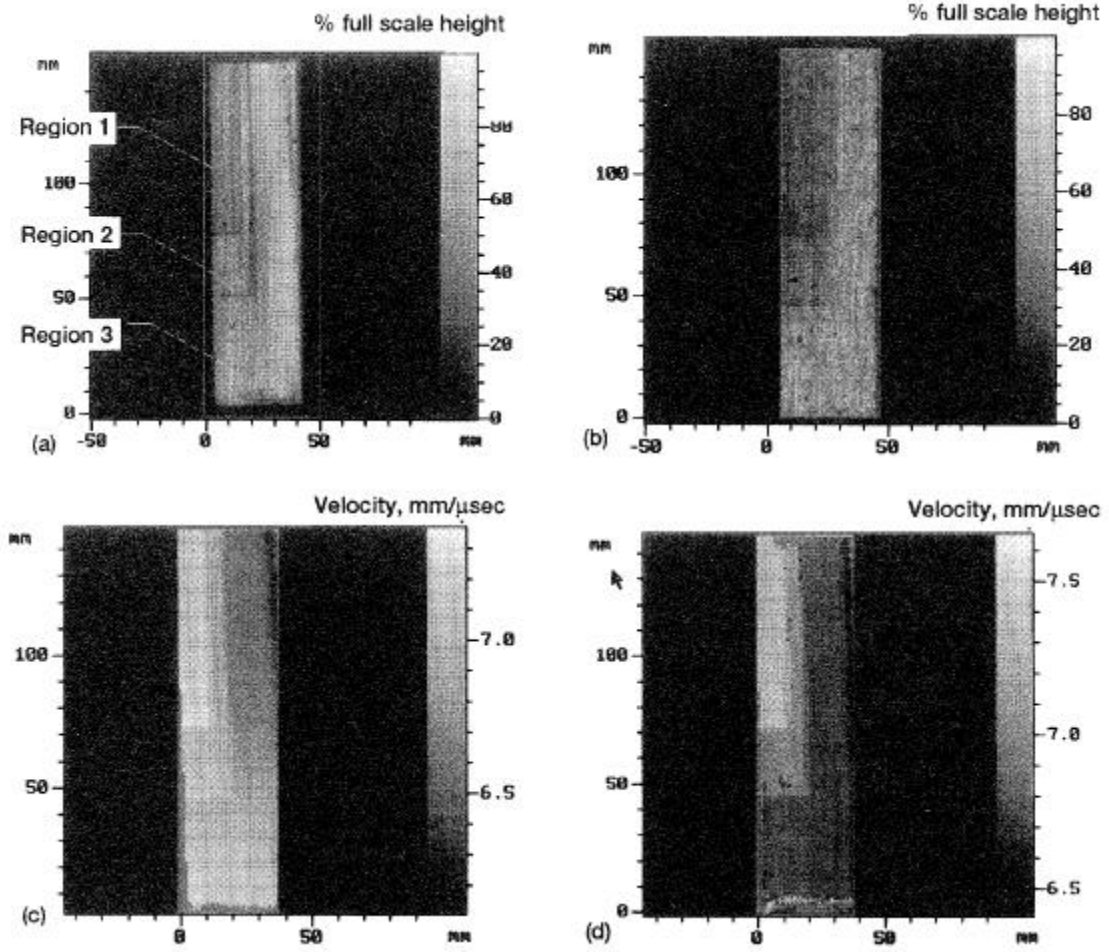


Fig. 6

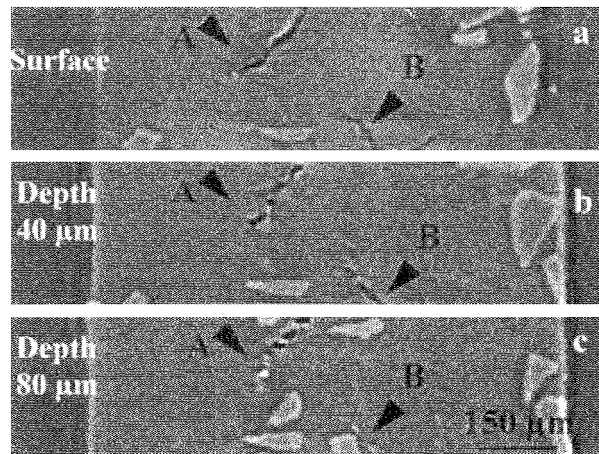


Fig. 7

MMC-Assess Publications

Volume 1: *Glossary of Terms specific to Metal Matrix Composites*

Volume 2: *Thermal Treatments of Age-hardenable Metal Matrix Composites*

Volume 3: *Metallographic Preparation of Metal Matrix Composites*

Volume 4: *X-Ray Computed Tomography on Metal Matrix Composites*

Volume 5: *Quality control and nondestructive tests in metal matrix composites*

Volume 6: *Machining guidelines of Al/SiC particulate MMC*

Volume 7: *Thermophysical Properties of Metal Matrix Composites*

Volume 8: *Guidelines for joining of metal matrix composites*

Volume 9: *Bonding and interface formation in Metal Matrix Composites*

Copyright: MMC-Assess Consortium, August 2000

Content: Y. D. Huang, L. Froyen, M. Wevers

Design: P. Prader

Contact: Insitute of Materials Science and Testing – Vienna University of Technology
mmc_assess@ewkmmc.tuwien.ac.at

Homepage: <http://mmc-assess.tuwien.ac.at/>